ELSEVIER

Thermochimica Acta 324 (1998) 95–107

thermochimica acta

Kinetics of irreversible melting of polyethylene crystals revealed by temperature modulated DSC[1]

Akihiko Toda[a,*], Chiyoko Tomita[a], Masamichi Hikosaka[a], Yasuo Saruyama[b]

[a] *Faculty of Integrated Arts and Sciences, Hiroshima University, 1-7-1 Kagamiyama, Higashi-Hiroshima 739, Japan*
[b] *Faculty of Textile Science, Kyoto Institute of Technology, Matsugasaki, Sakyo-ku, Kyoto 606, Japan*

Abstract

Temperature modulated differential scanning calorimetry (TMDSC) has been applied to study the irreversible melting kinetics of polyethylene crystals on heating. The apparent heat capacity obtained by TMDSC showed strong dependences on the applied frequency (modulation period) and on the heating rate. Considering the details of the melting kinetics, the dependence has been explained by a frequency response function similar to Debye's type with a characteristic time representing the melting kinetics. From the analysis, it has been confirmed that the 'reversing' heat flow extrapolated to $\omega \rightarrow 0$ is correspondent to the 'total' heat flow, when re-crystallization and re-organization are not significant during the melting process. It is further suggested that the characteristic time is related to the superheating effect seen in the 'total' heat flow. It is pointed out that the distribution of the melting points may be estimated by the deconvolution of the melting kinetics from the 'total' heat flow.

Keywords: Kinetics of melting; Polyethylene; Polymer crystals; Temperature modulated DSC

1. Introduction

We have recently proposed a new analyzing method of temperature modulated differential scanning calorimetry (TMDSC) applicable to irreversible transformation kinetics such as polymer crystallization and melting [1–5]. TMDSC [6–11] utilizes the response in heat flow, $\dot{Q}$, to a sinusoidal modulation in sample temperature, T_s, expressed as,

$$T_s = \overline{T}_s + \tilde{T}_s e^{i(\omega t+\epsilon)} \quad (1)$$

$$\dot{Q} = \overline{\dot{Q}} + \tilde{\dot{Q}} e^{i(\omega t+\delta)} \quad (2)$$

where $\overline{T}_s$ can be linear heating or cooling, $\overline{T}_s = \beta t$, or a constant temperature. Our new analyzing method is based on the behavior of an apparent heat capacity, $\Delta\tilde{C}e^{-i\alpha}$, determined from the response as,

$$\Delta\tilde{C}e^{-i\alpha} \equiv \Delta\tilde{C}' - i\Delta\tilde{C}'' \quad (3)$$

$$\Delta\tilde{C} \equiv \frac{\tilde{\dot{Q}}}{\omega\tilde{T}_s} \quad (4)$$

$$\alpha \equiv (\epsilon - \delta) - (\epsilon - \delta)_0 \quad (5)$$

where $(\epsilon-\delta)_0$ represents the baseline of the phase lag. We have suggested that the apparent heat capacity for the transformation processes should be expressed as,

$$\Delta\tilde{C}e^{-i\alpha} = mc_p + i\frac{1}{\omega}F'_T \quad (6)$$

where mc_p is given by the true heat capacity of sample and F'_T represents the response of the transformation

*Corresponding author. Tel.: +81-0-824-24-6558; fax: +81-0-824-24-0757; e-mail: atoda@ipc.hiroshima-u.ac.jp

[1]Presented in part at the 25th Conference of the North American Thermal Analysis Society, McLean, Virginia, September 7–9, 1997.

0040-6031/98/$ – see front matter
PII: S0040-6031(98)00527-9

process (i.e. temperature derivative of the transformation rate).

In the case of crystallization of polyethylene [1,2] and poly(ethylene terephthalate) (PET) [3,4], the apparent heat capacity showed a frequency response which indicates a constant F'_T independent of frequency:

$$\Delta\tilde{C}\mathrm{e}^{-i\alpha} = A + i\frac{B}{\omega} \tag{7}$$

where $A(>0)$ and $B(\lessgtr 0)$ are constants. The crystallization of polymers is characterized by the linear growth of lamellar crystals under high supercooling (>10 K), and hence the growth of crystals continues for a small temperature modulation (±0.2 K). Hence, the response to the temperature modulation should be given by the modulation of the growth rate. We have proposed the following expression of the process,

$$\Delta\tilde{C}\mathrm{e}^{-i\alpha} = mc_\mathrm{p} + i\frac{1}{\omega}\overline{F}_\mathrm{cryst}\frac{\mathrm{d}}{\mathrm{d}t}\ln(G/G_0) \tag{8}$$

where $\overline{F}_\mathrm{cryst}(>0)$ represents the exothermic heat flow of crystallization and $\mathrm{d}/\mathrm{d}t\ln(G/G_0)$ ($\lessgtr 0$) the temperature dependence of linear growth rate of crystals. Utilizing the imaginary part and the exothermic heat flow of crystallization, we have successfully determined the temperature dependence of growth rate, the results of which were in good agreement with the values obtained by direct measurements of growth rate by microscopy.

In a preceding paper [5], we have also examined the irreversible melting of PET crystals on heating ($\mathrm{d}T_\mathrm{s}/\mathrm{d}t>0$). The experimental results showed a strong dependence of the apparent heat capacity on the applied frequency of modulation and on the heating rate, β. The dependence could be approximated by a frequency response function of Debye's type as,

$$\Delta\tilde{C}\mathrm{e}^{-i\alpha} \simeq C + \frac{D}{1 + i\omega t(\beta)} \tag{9}$$

where $C(>0)$ and $D(>0)$ are constants. In order to explain the dependence, mc_p or F'_T in Eq. (6) needs to be frequency dependent. The true heat capacity, mc_p, can be frequency dependent and undergo a relaxation process such as glass transition giving a negative imaginary part of mc_p as a consequence of irreversibility [12,13]. However, since the transformation is not a relaxation process, the frequency response should be ascribed to the frequency response of the melting kinetics to temperature modulation. In the preceding paper [5], we have modelled the melting kinetics and obtained the expression of the apparent heat capacity approximated as,

$$\Delta\tilde{C}\mathrm{e}^{-i\alpha} \simeq mc_\mathrm{p} + \frac{(-\overline{F}_\mathrm{melt}/\beta)}{1 + i\omega\tau(\beta)} \tag{10}$$

$$\tau(\beta) \propto \beta^x,\ -1 \le x \le 0 \tag{11}$$

where $\overline{F}_\mathrm{melt}(<0)$ represents pure endothermic heat flow of melting and $\tau(\beta)$ represents the characteristic time of melting kinetics and can be treated as a measure of the time required for the complete melting of crystallites (see Appendix A for the exact formulas).

Before proceeding to the purpose of the present paper, we shortly review the characteristics of the melting of polymer crystals [14] as typically seen in the melting of PET crystals. Polymer crystals comprise small crystallites which are quasi-stable and have a continuous distribution of the non-equilibrium melting points owing to the distributions of the thin lamellar thickness and of molecular weight. The resulting successive melting of the crystallites is the primary cause of the characteristic feature of a broad melting peak (≃50 K) on heating. In the theoretical approach in Ref. [5], we have assumed a quasi-steady state of the irreversible melting, and calculated the response of the irreversible melting kinetics to temperature modulation during heating run (Appendix A). It is noted here that the irreversible melting under the condition of heating only, $\mathrm{d}T_\mathrm{s}/\mathrm{d}t>0$, is distinguished from the reversible processes of melting and crystallization expected around the melting point for a quasi-isothermal measurement [15,16]. Owing to the quasi-stable nature of the crystallites, re-crystallization and/or re-organization also set in along with the irreversible melting on heating. This effect has been recognized as a shift of the melting peak to higher temperature for slower heating rate. If we utilize the relation between the apparent heat capacity and the 'total' heat flow suggested in Eq. (10) and the relatively insensitive nature of crystallization to temperature modulation, it has been shown that the 'total' heat flow can be separated into pure endothermic heat

flow of melting and pure exothermic heat flow of re-crystallization and re-organization [5].

In the present paper, we examine the irreversible melting of polyethylene crystals on heating. The melting of polyethylene crystals has the following characteristics which differ from the melting typically seen in PET crystals. Firstly, polyethylene crystals have a relatively narrow melting peak ($\simeq$10 K), and hence it is required to examine the applicability of our approach assuming a uniform distribution of the melting points. Secondly, it is known that the re-crystallization and re-organization are not significant if the sample is crystallized by slow cooling [14,17]. If it is the case, the 'total' heat flow obtained by TMDSC (or by a conventional DSC) represents true endothermic heat flow of melting under the condition that the heating rate is not influenced by the heat flow. Then, the 'total' heat flow should be correspondent with $\overline{F}_{\mathrm{melt}}$ obtained from the frequency response of the apparent heat capacity suggested in Eq. (10). Lastly, because of the relatively sharp melting peak, a superheating effect is seen in a conventional DSC with fast heating as the shift of the melting peak to higher temperature for faster heating rate [17]. This effect must be related to the characteristic time of melting, τ, obtained by TMDSC. Those characteristics expected for the melting of polyethylene crystals needs to be investigated, in order to confirm the applicability of the expression shown in Eq. (10) to the irreversible melting kinetics of polymer crystals.

2. Experimental

The DSC 2920 Module controlled with Thermal Analyst 2200 (TA Instruments) and equipped with a TA RMX Utility was used for all measurements. Nitrogen gas with a flow rate of 40 ml min^{-1} was purged through the cell. The phase, ϵ and δ, were calculated from the raw data of sample temperature and of heat flow.

Modulation period of 24–100 s was examined with the modulation amplitude adjusted for the condition of heating only, $\mathrm{d}T_{\mathrm{s}}/\mathrm{d}t > 0(\tilde{T}_{\mathrm{s}} < \beta/\omega)$. As a preliminary experiment, we have examined different amplitude of temperature modulation, as shown in Fig. 1. The apparent heat capacity during the melting process was affected by the choice of the amplitude larger than

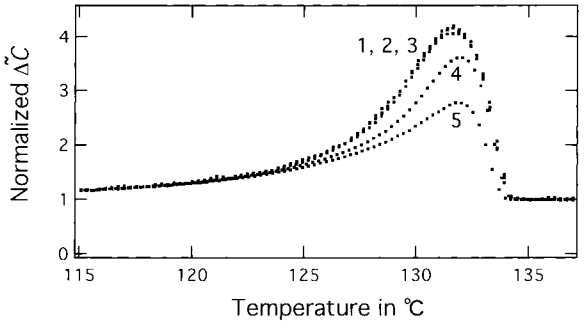

Fig. 1. Plots of the magnitude of the apparent heat capacity during the melting process of polyethylene crystals by heating runs at 0.6 K min^{-1} with different amplitude of temperature modulation $\tilde{T}_{\mathrm{s}}$: (1) 0.020, (2) 0.042, (3) 0.100, (4) 0.300 and (5) 0.700 K. The modulation period was 28 s. The condition of heating is only satisfied when $\tilde{T}_{\mathrm{s}} \leq 0.044$ K for the modulation period. The data points are plotted at the interval of the applied modulation period.

what is given by the above condition. In order to assure self-consistency, we have employed the condition of heating only, even though the amplitude becomes quite small for slower heating rate with shorter modulation period; the minimum amplitude was 0.012 K for the heating rate of 0.2 K min^{-1} and the period of 24 s. Since we are concerned with the response to a periodic modulation of sinusoidal profile, Fourier integral at the applied modulation frequency has been utilized to calculate the magnitude and phase of the signals of sample temperature and of heat flow. Hence, the improvement of the quality of the data can be expected by the procedure, even though the signal/noise ratio became worse for such a small amplitude, as typically shown in Fig. 7(a).

The DSC runs of the present experiment consisted of cyclic heating and cooling runs with different modulation periods and heating rates for a single sample. The polyethylene sample of 4.01 mg was NIST SRM1475 of M_{w}=5.2×10^4 and $M_{\mathrm{w}}/M_{\mathrm{n}}$=2.9. The cooling runs were at the rate of 2.0 K min^{-1} from the melt kept at 150°C, and the heating runs were from 90°C at the rate in the range of 0.2–2.0 K min^{-1}. In the data analysis of TMDSC, the apparent heat capacity of each run with different modulation periods was normalized by the value of molten polyethylene at 140°C and hence the apparent heat capacity has been automatically calibrated for different modulation periods. The baseline of the phase lag, $(\epsilon-\delta)_0$, was set to follow

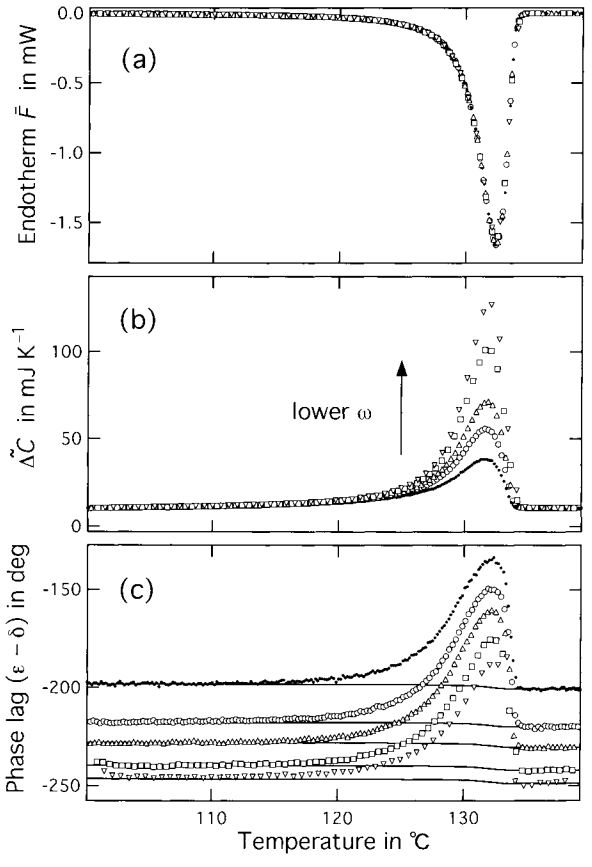

Fig. 2. Raw data of TMDSC showing the frequency dependence of the melting process of polyethylene crystals by heating runs at 0.4 K min^{-1}: (a) endothermic heat flow $\overline{F}$ obtained by a conventional baseline subtraction without the 'reversing' heat flow, (b) the magnitude of the apparent heat capacity $\Delta\tilde{C}$ after the correction for different modulation periods and (c) phase lag $(\epsilon-\delta)$. The symbols represent the following modulation periods: 28 (●), 40 (○), 52 (△), 76 (□) and 100 s (▽). In (c), the lines represent the baseline, $(\epsilon-\delta)_0$. The data points are plotted at the interval of the applied modulation period.

the change in the degree of crystallinity estimated from the integration of the endothermic heat flow, as shown in Fig. 2(c). The choice of the baseline will not be crucial because the melting peaks in the phase lag were large enough. The baseline of the endothermic heat flow was not corrected for the subtraction of the contribution of heat capacity (the 'reversing' heat flow, $-\beta\Delta\tilde{C}$), because the 'reversing' heat flow contains the information of the endothermic heat flow of melting itself, as suggested by Eq. (10).

3. Results and discussion

3.1. Frequency and heating rate dependence of the apparent heat capacity

Fig. 2 shows the endothermic heat flow, $\overline{F}$, the magnitude of the apparent heat capacity, $\Delta\tilde{C}$, and the phase lag, $(\epsilon-\delta)$, on heating at the rate of 0.4 K min^{-1} for different periods of modulation. Fig. 3 shows the real and imaginary parts of the apparent heat capacity calculated from $\Delta\tilde{C}$ and $(\epsilon-\delta)$ with the appropriate baseline of $(\epsilon-\delta)_0$ as shown in Fig. 2. Both the real and imaginary parts of the apparent heat capacity showed strong dependence on frequency, while the heat flow was not affected by the change of modulation period. The frequency response of the apparent heat capacity has been examined for different heating rates. The frequency dependence at the same temperature of 131.0°C is compared in Fig. 4 where the curved lines represent the fittings of the expected response functions of Eqs. (A.11), (A.16)

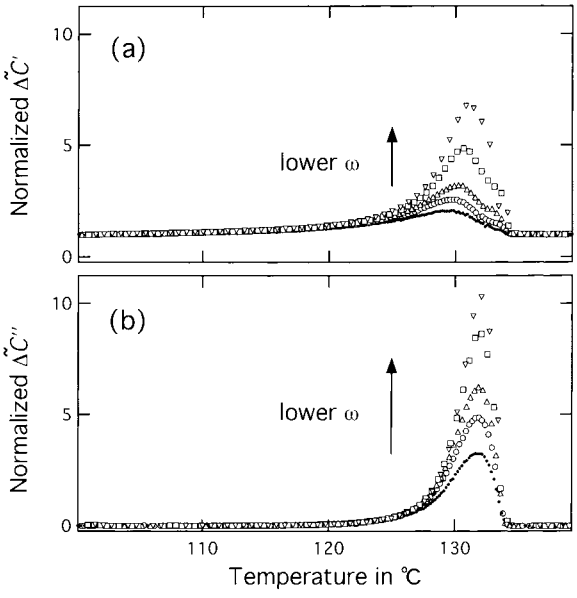

Fig. 3. Frequency dependence of (a) the real part $\Delta\tilde{C}'$ and (b) the imaginary part $\Delta\tilde{C}''$ of the apparent heat capacity obtained by the data shown in Fig. 2. The symbols represent the following modulation periods: 28 (●), 40 (○), 52 (△), 76 (□) and 100 s (▽). The value of the apparent heat capacity was normalized by that of molten polyethylene at 140°C. The data points are plotted at the interval of the applied modulation period.

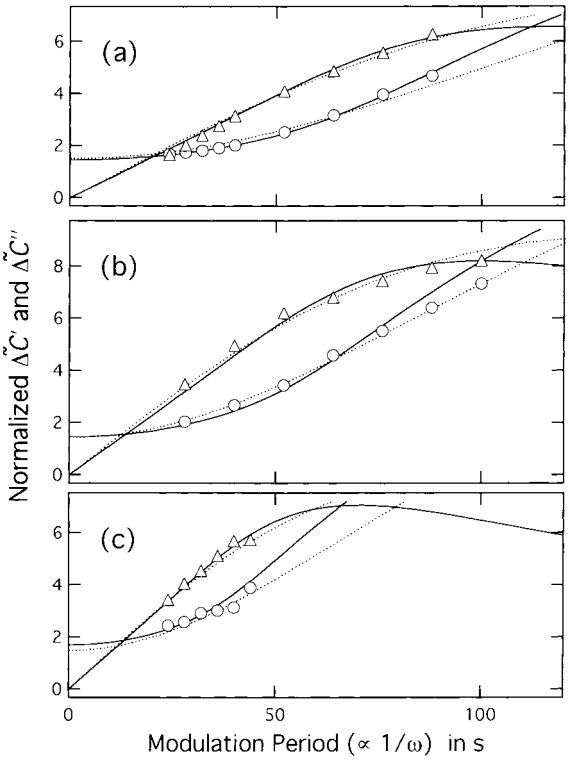

Fig. 4. Plots of the real (○) and imaginary (△) parts of the (normalized) apparent heat capacity during the melting process of polyethylene against modulation periods. The data at 131.0°C were taken from the heating runs of the following rates: (a) 0.2, (b) 0.6 and (c) 1.5 K min^{-1}. The solid and broken lines are the plots of Eqs. (A.14) and (A.11) (or Eq. (A.16)), respectively, with the adjustable parameters of c_p, ϕ_0 and τ_1 or τ_0 (or τ_2).

and (A.14) with the adjustable parameters of c_p, ϕ_0 and τ (Appendix A). In Fig. 4, it is clearly seen that the peak in the plots of the imaginary parts moves to slower modulation period for faster heating. This change indicates that the characteristic time, τ, becomes shorter for faster heating rate. All those behaviors have also been confirmed for the melting of PET crystals [5] and provided a contrast to the frequency response in polymer crystallization as expressed in Eq. (7).

Fig. 5 shows the results of fitting to Eqs. (A.11) and (A.16) and to Eq. (A.14) of the real and imaginary parts of the apparent heat capacity obtained for different heating rates at the temperatures of 128°, 130° and 132°C. As shown in Fig. 5, the data points could be fitted to both the response functions; we need to examine the dependence on heating rate of the characteristic time, τ, to specify which response function explains the experimental results better. Fig. 6(a) shows the dependence on heating rate of the characteristic time, τ, obtained by a fitting, such as that shown in Fig. 4. The dependence can be approximated as $\tau \propto \beta^{-0.5}$ at higher temperature around the melting peak, while the exponent becomes smaller than 0.5 for lower temperature. Therefore, it seems that the response functions of $f_1(\omega)$ of Eq. (A.14) explains the behavior at higher temperatures, while the dependence approaches to $f_0(\omega)$ of Eq. (A.11) at lower temperatures. The change of the frequency response function indicates the shift of the superheating dependence of the melting rate coefficient from a constant rate to the rate linearly dependent on superheating as temperature increases. As shown in Fig. 6(b), the absolute values of τ also change with temperature: shorter τ at lower temperatures. The constant melting rate coefficient does not mean weaker dependence on superheating, but it represents a sudden rise of the melting rate coefficient just above the non-equilibrium melting points. Therefore, from the results of the temperature dependence of τ and the change in the superheating dependence with temperature, it can be said that the melting process must be more easily advanced for the crystallites having lower melting points. The melting of PET crystals examined previously also showed a behavior similar to it [5]; we confirmed the temperature dependence of τ and the shift of the melting kinetics from the linear dependence of $f_1(\omega)$ as shown in Eq. (A.14) to the exponential dependence of $f_2(\omega)$ in Eq. (A.16) with increasing temperature.

The analysis discussed above proves the applicability of our new approach to the melting of polyethylene crystals having relatively narrower melting peak. In order to apply the present model, the requirement of a quasi-steady state must be satisfied (Appendix B). The first condition of the requirement in Appendix B (Eq. (B.20)) can be judged by plotting Lissajous diagram of the modulated heat flow against the modulated sample temperature [15,16], as shown in Fig. 7 where the two cycles of the data during the melting peak are plotted. Considering the divergence from a closed loop in Fig. 7(d), for the fastest heating rate of 2.0 K s^{-1}, the modulation period of 36 s seems to exceed the limit. Since the number of data points

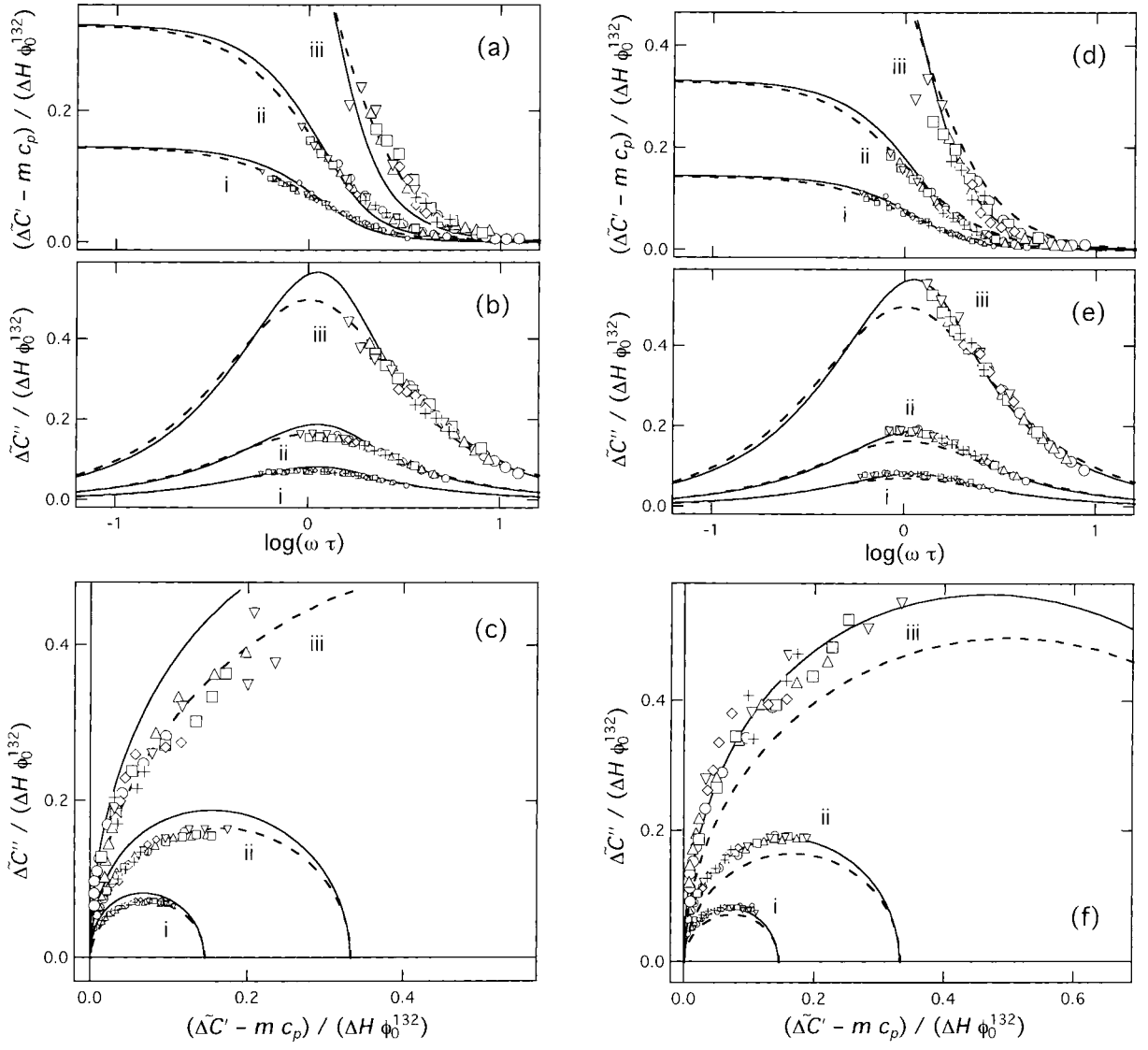

Fig. 5. The real and imaginary parts of the apparent heat capacity such as shown in Fig. 4 taken at (i) 128.0, (ii) 130.0 and (iii) 132.0°C for different heating rates. The symbols represent the following heating rates: 0.2 (○), 0.4 (△), 0.6 (□), 1.0 (▽), 1.5 (◇) and 2.0 K min^{-1} (+). The broken and solid lines represent the plots of Eq. (A.11) (or Eq. (A.16))Eq. (A.14), respectively. With the adjustable parameters of c_p, ϕ_0 and τ_0 (or τ_2) or τ_1, the data points were fitted to the broken lines in (a)–(c) and to the solid lines in (d)–(f).

within the melting peak becomes smaller for faster heating rate and for longer modulation period, we had to choose shorter modulation periods for faster heating rate as shown in Fig. 4. If we carefully choose the condition to include the cycles of modulation large enough, we can apply the present analysis based on the assumption of the quasi-steady state (Appendix B). It is further noted that the present analysis does not require the linear response of the melting kinetics which should contain higher harmonics of Eq. (A.4), while the linear response concerns the apparent heat capacity. In Fig. 8, it is seen that the non-linearity of the response is not so strong as in the case of the melting of PET crystals ($F_2/F_1 \sim 0.08$) [5].

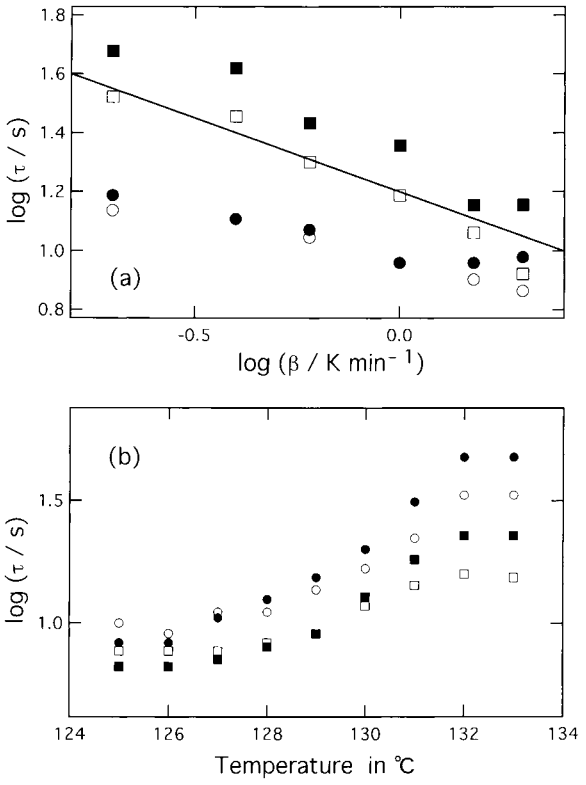

Fig. 6. Logarithmic plots of the characteristic time τ chosen for the fitting such as shown in Fig. 4 against (a) heating rate β and (b) temperature. In (a), the symbols represent the values determined for the temperatures of 129.0 (○, ●) and 133.0°C (□, ■), and in (b) the values were for the heating rate of 0.2 (○, ●) and 1.0 K min^{-1} (□, ■). The open and filled symbols correspond to the fitting to Eqs. (A.14) and (A.11) (or Eq. (A.16)) of the apparent heat capacity, respectively. The slope of the solid line in (a) is −0.5.

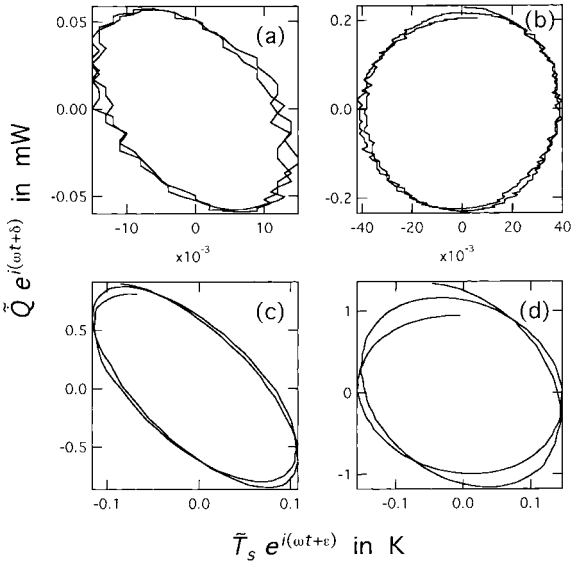

Fig. 7. Lissajous diagrams of the modulation component of heat flow during the melting peak plotted against that of sample temperature. The two cycles of the modulation are plotted. The heating rate and the modulation period of TMDSC are the followings: (a) 0.2 K min^{-1} and 28 s, (b) 0.2 K min^{-1} and 88 s, (c) 2.0 K min^{-1} and 24 s and (d) 2.0 K min^{-1} and 36 s.

3.2. The 'reversing' heat flow and the 'total' heat flow

Following the expression of Eq. (10), pure endothermic heat flow of melting, $\overline{F}_{\mathrm{melt}}$, is related to the extrapolation of the apparent heat capacity to $\omega \rightarrow 0$. So called 'reversing' heat flow of $-\beta\Delta\tilde{C}$ is

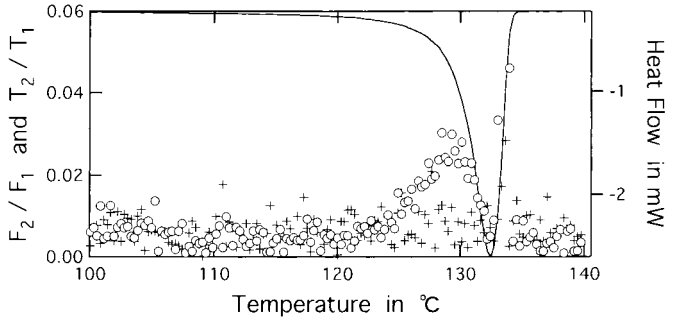

Fig. 8. Plots of the ratio of the amplitude of the first and second harmonics of the response in heat flow, F_2/F_1 (○), and that of sample temperature, T_2/T_1 (+), during the melting peak seen in the heat flow (curved line). The heating rate was 0.6 K min^{-1}. The modulation period was 28 s.

then expressed as,

$$-\beta\Delta\tilde{C}(\omega \to 0) = -\beta mc_p + \overline{F}_{melt} \quad (12)$$

It is known that re-crystallization or re-organization accompanying the melting is not significant for the melting of polyethylene crystals, if the crystals are prepared by slow cooling [14,17]. In the present measurements, the cooling rate was 2.0 K min^{-1} and will be slow enough. Therefore, $\overline{F}_{melt}$ determined from the extrapolation should correspond to the underlying endothermic heat flow, $\overline{F}$, appearing in the 'total' heat flow expressed as, $\dot{Q} = -\beta mc_p + \overline{F}$, under the condition that the heat flow does not significantly influence the heating rate of the sample temperature. Then, the 'total' heat flow must be correspondent with the 'reversing' heat flow extrapolated to $\omega \to 0$,

$$\overline{\dot{Q}} = -\beta\Delta\tilde{C}(\omega \to 0) \quad (13)$$

Fig. 9 shows the comparison of $\overline{\dot{Q}}$ and $-\beta\Delta\tilde{C}(\omega \to 0)$ determined from the adjustable parameters of the fittings such as shown in Fig. 4. The agreement between them is satisfactorily and confirms the relation of Eq. (13) when the exothermic heat flow of re-crystallization or re-organization is not significant.

In Fig. 9, the heat capacity, mc_p, determined by the fitting is also plotted. The heat capacity seems to be higher in the temperature range of melting than that of the melt. Such an inverted relationship near the melting point has been reported by Gaur and Wunderlich [18] and also seen during crystallization process [1,2]. If we utilize a light modulated DSC [19,20,21], we can apply shorter modulation period ($\sim$2 s) and the real part of the apparent heat capacity levels off because of the $1/\omega$ dependence of the second term of Eq. (10). Hence, the heat capacity, mc_p, can be directly determined by this technique and the results were similar in its temperature profile to the present results.

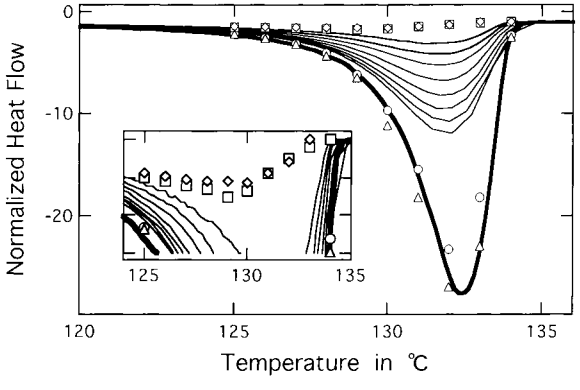

Fig. 9. Plots of the 'total' heat flow $\overline{\dot{Q}}$ (thick line) and the 'reversing' heat flow (thin lines) obtained with the modulation periods of 24–100 s for the heating rate of 0.4 K min^{-1}. Symbols represent the 'reversing' heat flow extrapolated to $\omega \to 0$, $-\beta[mc_p + \Delta H\phi_0]$, (○, △) and the true heat capacity mc_p, (□, ◇) determined by the fitting to Eqs. (A.14) and (A.11) (or Eq. (A.16)) of the apparent heat capacity, respectively. The heat flow was normalized by the 'total' heat flow of molten polyethylene at 140°C.

3.3. Characteristic time τ and the superheating effect seen in DSC

Fig. 10(a) shows the superheating effect appearing as the shift of the melting peak to higher temperature for faster heating rate. If the melting is instantaneous, the heat flow will be correspondent to the distribution of the melting points, $\phi_0(T_m)$, with the melting kinetics represented as $\dot{\psi}$ having a finite value of the characteristic time. This type of temperature shift can also be caused by the response of DSC with a relaxation time represented as, $\tau_{DSC} \equiv C_p/K$, where $1/K$ is the thermal resistance of the DSC [22]. Therefore, the heat flow of Eq. (B.18) needs to be further convoluted with $e^{-t/\tau_{DSC}}$. We have estimated the value of $\tau_{DSC} \sim 3.7$ s from the tail of the melting peak of Indium. Fig. 10(b) and (c) show the results considering the convolutions of $\phi_0(T_m)$ with $\dot{\psi}$ and $e^{-t/\tau_{DSC}}$ under the assumption that the heat flow data of the slowest heating rate (0.2 K min^{-1}) represents the true $\phi_0(T_m)$. In Fig. 10(b), the constant melting rate coefficient R_0 is assumed and hence the development of the melting is represented by Eq. (A.10). The characteristic time τ_0 of 26 s estimated from Fig. 6(a) was chosen to be independent of heating rate (Eq. (A.9)). On the other hand, in Fig. 10(c), the linear dependence on supercooling (Eq. (A.13)) is assumed and the characteristic time was chosen to satisfy the heating rate dependence of Eq. (A.12). It is noted that the convolution with

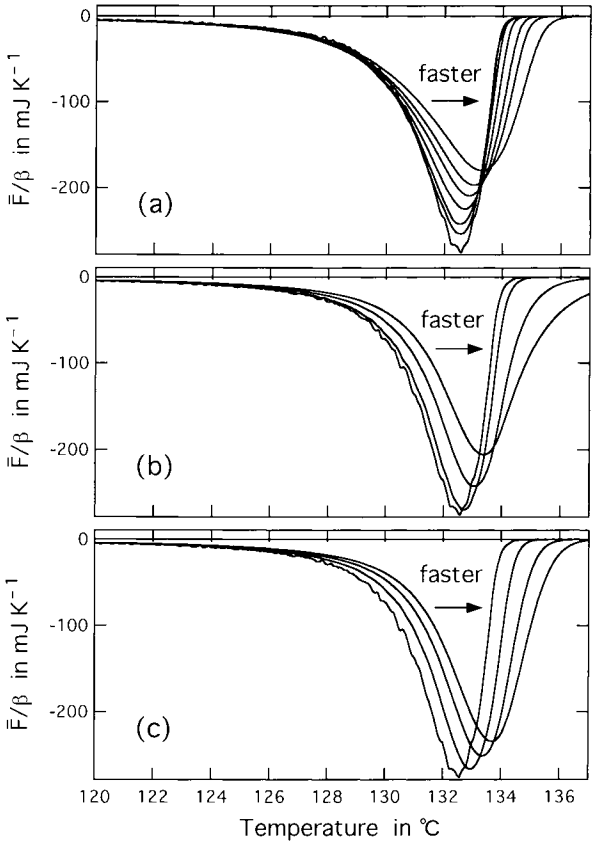

Fig. 10. (a) Plots of endothermic heat flow divided by heating rate, $\overline{F}/\beta$, during the melting process of polyethylene crystals for different heating rates of 0.2, 0.4, 0.6, 1.0, 1.5, 2.0, and 3.0 K min^{-1}. Temperature modulation was not applied. (b) Convolution of an initial distribution of the melting points, $\phi(0, T_m)$, approximated by $-\overline{F}/(\beta\Delta H)$ of 0.2 K min^{-1} with the development of the melting for the constant melting rate coefficient of Eq. (A.10) with a characteristic time of 26 s. The heating rate is 0.2, 0.4, 1.5 and 3.0 K min^{-1}. (c) The convolution for a linear dependence of the melting rate coefficient on superheating (Eq. (A.13)). The heating rate and the corresponding characteristic time defined by Eq. (A.12) are (0.2, 100), (0.4, 71), (1.5, 37) and (3.0, 26) in K min^{-1} and s.

$e^{-t/\tau_{DSC}}$ did not significantly influence the results because the relaxation time of DSC is much shorter than the characteristic time of the melting kinetics. Both the plots in Fig. 10(b) and (c) well reproduce the range of temperature shift of the melting peak, but the agreement of the profile of melting endotherm with the experimental results is not satisfactorily. In the calculation, we have assumed a single characteristic time to make the convolution, but it is apparent from Fig. 6(b) that the characteristic time undergoes a substantial change with temperature. If the change in τ is concerned, Eq. (B.18) is not applicable, and hence further study will be required on this subject.

4. Conclusion

With the apparent heat capacity of complex quantity obtained by TMDSC, we have examined the irreversible melting kinetics of polyethylene crystals on heating. Considering the quasi-stable nature of polymer crystals and the distribution of the non-equilibrium melting points, we have suggested the frequency response functions similar to Debye's type with the characteristic time being dependent on heating rate. The experimental data showed strong dependences on frequency and on heating rate. The dependences have been analyzed by the response functions with the characteristic time describing the melting kinetics. It is further suggested that the apparent heat capacity is related to the underlying heat flow of melting; namely, the 'reversing' heat flow extrapolated to $\omega\rightarrow 0$ corresponds to the underlying heat flow of melting. In the case of polyethylene, since recrystallization and re-organization are not significant for the crystals formed on slow cooling, it has been confirmed that the 'total' heat flow representing the heat flow of melting actually corresponds to the extrapolated 'reversing' heat flow. The agreement supports the applicability of our new approach. When re-crystallization and re-organization become appreciable as in the case of poly(ethylene terephthalate), we are able to separate the endothermic heat flow of melting from the exothermic heat flow of re-crystallization and re-organization, utilizing the difference in the sensitivity of those processes to temperature modulation [5]. We have also suggested the relationship between the characteristic time determined by TMDSC and a temperature shift of the melting peak for faster heating rate, known as superheating effect. Utilizing the relationship, it may be possible to estimate the distribution of the melting points from the endothermic heat flow of melting by the deconvolution of the melting kinetics. This technique may also be applicable to the purity analysis of other non-polymeric systems.

Acknowledgements

This work was partly supported by NEDO International Joint Research Program.

Appendix A

Modelling of the melting kinetics of polymer crystals

We briefly summarize the modelling suggested in the preceding paper [5]. In order to model the melting process of an aggregate of crystallites having a distribution of the melting points, we consider the fraction of crystallites, $\phi(t, T_m)\,dT_m$, having the melting temperature in the range from T_m to T_m+dT_m. The total crystallinity, $\Phi(t)$, is then expressed by the fractions as,

$$\Phi(t) = \int_0^\infty dT_m \phi(t, T_m) \tag{A.1}$$

The change in the fraction, $\phi\ (t, T_m)$, is described by the total melting rate coefficient, R, of the fraction as,

$$\phi(\Delta t, T_m) = \phi(0, T_m)\exp\left[-\int_0^{\Delta t} R\,dt'\right] \tag{A.2}$$

The endothermic heat flow of melting, $F_{melt}(t)$, is given by the time derivative of the total crystallinity multiplied by the enthalpy change, ΔH, of the system as,

$$F_{melt}(t) = \Delta H \frac{d\Phi}{dt} \tag{A.3}$$

In order to calculate the steady response in heat flow, we suppose a hypothetical situation of a uniform distribution of the initial fractions, $\phi\ (0, T_m)=\phi_0$. For the uniform distribution, the response of heat flow to a sinusoidal modulation of temperature should be in a steady state and can be represented by Fourier series expressed as,

$$F_{melt}(t) = \overline{F}_{melt} + F'_T(\omega)\tilde{T}_s e^{i\omega t} + \dots \tag{A.4}$$

$$\overline{F}_{melt} = -\beta\Delta H\phi_0 \tag{A.5}$$

$$F'_T(\omega)\tilde{T}_s = \beta\phi_0 \int_{-\infty}^{\infty} dt\, e^{-i\omega t} F_{melt}(t) \tag{A.6}$$

Hence, the response of the melting kinetics, $F'_T(\omega)$, is given by Fourier transform of the modulated heat flow of melting, $F_{melt}(t)$, at the applied modulation frequency, ω (Eq. (B.6) in Appendix B). Here, it is reminded that the apparent heat capacity of complex quantity is defined as a coefficient of the change in temperature in the expression of heat flow as,

$$\dot{\tilde{Q}} e^{i(\omega t+\delta)} = -\Delta\tilde{C} e^{-i\alpha} \frac{d}{dt}\tilde{T}_s e^{i(\omega t+\epsilon)} \tag{A.7}$$

and hence the contribution of the melting kinetics, $f(\omega)$, to the apparent heat capacity ($\Delta\tilde{C}e^{-i\alpha} = mc_p + f(\omega)$) is given by,

$$f(\omega) \equiv \frac{i}{\omega} F'_T(\omega) \tag{A.8}$$

as shown in Eq. (6).

The modulation in temperature influences the melting rate coefficient, $R(\Delta T)$, being a function of superheating, $\Delta T(\equiv T_s - T_m)$, and consequently the time development of $\phi(t, T_m)$. Assuming a linear expansion of $R(\Delta T)$ and $\phi\ (t, T_m)$ about temperature modulation of small amplitude, we can calculate the response, $F'_T(\omega)$, and evaluate the contribution of the kinetic response to the apparent heat capacity, $f(\omega)$. We have examined three different dependences on superheating of the melting rate coefficient: (1) constant melting rate coefficient, R_0, (2) linear dependence, $R_1=a\Delta T$, and (3) exponential dependence, $R_2 \propto e^{c\Delta T}$. The melting kinetics of each case is described by a characteristic time, τ, which can be dependent on heating rate, β. The calculated results are summarized as follows.

(i) Constant melting rate coefficient: R_0

$$\tau_0 \equiv 1/R_0 \tag{A.9}$$

$$\phi(\Delta t) = \phi_0 \exp\left(-\frac{\Delta t}{\tau_0}\right) \tag{A.10}$$

$$f_0(\omega) = \frac{\Delta H\phi_0}{1 + i\omega\tau_0} \tag{A.11}$$

(ii) Linear dependence: $R_1=a\Delta T$

$$\tau_1 \equiv \left(\frac{1}{2\alpha\beta}\right)^{1/2} \tag{A.12}$$

$$\phi(\Delta t) = \phi_0 \exp\left(-\left(\frac{\Delta t}{2\tau_1}\right)^2\right) \tag{A.13}$$

$$f_1(\omega) = \frac{\Delta H \phi_0}{\omega\tau_1}\left\{ e^{-(\omega\tau_1)^2} \times \int_0^{\omega\tau_1} e^{x^2} dx - i\frac{\sqrt{\pi}}{2}(1 - e^{-(\omega\tau_1)^2}) \right\} \quad (A.14)$$

The frequency response of f_1 is similar to that of f_0 as a function of $\omega\tau$, as shown in Fig. 5.

(iii) Exponential dependence: $R_2 \propto e^{c\Delta T}$

$$\tau_2 \equiv \frac{1}{\beta c} \quad (A.15)$$

$\phi(\Delta t)$: nearly stepwise at $\Delta t \sim \tau_2$

$$f_2(\omega) \simeq \frac{\Delta H \phi_0}{1 + i\omega\tau_2} \quad (A.16)$$

As shown above, the melting kinetics, namely the change in the crystallinity of a fraction, $\phi(\Delta t)$, is well described by the characteristic time, τ, which is dependent on the heating rate, β, as $\tau \propto \beta^x$ with $-1 \leq x \leq 0$. It is also noted that, from Eqs. (A.5), (A.11), (A.14) and (A.16), we can confirm the relationship between the underlying endothermic heat flow and the apparent heat capacity, explicitly shown in Eq. (10).

Appendix B

Necessary condition for the quasi-steady state approximated by a uniform distribution of the melting points, $\phi_0(T_m)$ ($\equiv\phi(0,T_m)$)$=\phi_0$

In a general expression of the modulated heat flow, $F_{melt}(t)$, with the change in $\phi_0(T_m)$, both of the underlying heat flow, $\overline{F}_{melt}(t)$, and the modulation component, $F'_T(t,\omega)$, must be time (temperature) dependent, and the heat flow is expressed as,

$$F_{melt}(t) = \overline{F}_{melt}(t) + F'_T(t,\omega)\tilde{T}_s e^{i\omega t} + \ldots \quad (B.1)$$

We consider Fourier transform of $F_{melt}(t)$ expressed as,

$$G(\omega') = \int_{-\infty}^{\infty} dt\, e^{-i\omega' t} F_{melt}(t) = \overline{G}(\omega') + \tilde{T}_s G'_T(\omega' - \omega, \omega) + \ldots \quad (B.2)$$

$$\overline{G}(\omega') \equiv \int_{-\infty}^{\infty} dt\, e^{-i\omega' t}\overline{F}_{melt}(t) \quad (B.3)$$

$$G'_T(\omega', \omega) \equiv \int_{-\infty}^{\infty} dt\, e^{-i\omega' t} F'_T(t,\omega) \quad (B.4)$$

In a particular case of the uniform distribution of ϕ_0 (T_m)$=\phi_0$, the melting kinetics is in steady state, and hence $\overline{F}_{melt}$ and $F'_T(\omega)$ keep constant values independent of time. Then, Fourier transform of the heat flow will be represented as,

$$G(\omega') = \overline{F}_{melt}\delta(\omega') + \tilde{T}_s F'_T(\omega)\delta(\omega' - \omega) + \ldots \quad (B.5)$$

Therefore, $F'_T(\omega)$ is given by Fourier transform of F_{melt} at the modulation frequency ω as,

$$\tilde{T}_s F'_T(\omega) = \overline{F}_{melt}\frac{G(\omega)}{G(0)}\left(= \overline{F}_{melt}\frac{G'_T(0,\omega)}{\overline{G}(0)}\right) \quad (B.6)$$

In the present analysis, we have assumed the steady state of the melting kinetics with the uniform distribution of the melting points, $\phi_0(T_m)=\phi_0$. Since we are concerned with the irreversible melting on heating, namely an irreversible transformation process, the process cannot be in the steady state in the long run with the actual distribution of the melting points, and hence we must consider whether the process can be approximated as a quasi-steady state or not. In the present case of the successive melting of crystallites with a broad melting peak, the assumption of the quasi-steady state is justified, if the profile of $G'_T(\omega', \omega)$ in the plot against ω' is not influenced by the applied frequency. This condition is expressed as,

$$G'_T(\omega', \omega) = g(\omega')h(\omega) \quad (B.7)$$

If it is the case, the frequency dependence of $f(\omega) = i/\omega F'_T(t,\omega)$ is determined by $1/\omega\ h(\omega)$ which corresponds to the results for the case of $\phi_0(T_m)=\phi_0$, as shown below.

In order to calculate Fourier transform of Eqs. (B.2)–(B.4), we need the detailed expression of $F_{melt}(t)$. Utilizing Eq. (A.3), $F_{melt}(t)$ is given by the melting rate coefficient, $R(\Delta T)$, and the crystal-

linity of fractions, ϕ (t,T_m), as,

$$F_{melt}(t) = \Delta H \frac{d}{dt}\int_0^\infty dT_m \phi(t, T_m) \quad (B.8)$$

$$= -\Delta H \int_0^\infty dT_m R(\Delta T)\phi(t, T_m)$$

When a temperature modulation is applied, we need to consider the response of $R(\Delta T)$ and $\phi(t, T_m)$. If the modulation amplitude is small enough, we can reasonably assume an expansion about the modulation components represented as,

$$R(\Delta T) = R(\beta\Delta t) + R'(\beta\Delta t)\tilde{T}_s e^{i\omega t_0}(e^{i\omega\Delta t} - 1) + \ldots \quad (B.9)$$

$$\phi(\Delta t, t_0) = \phi_0(t_0)\psi(\Delta t) \quad (B.10)$$

$$\psi(\Delta t) \equiv \begin{cases} 1 & \text{for } \Delta T < 0 \\ e^{-\int_0^{\Delta t} dx R(\beta x)}\left[1 - \tilde{T}_s e^{i\omega t_0}\int_0^{\Delta t} dx R'(\beta x)(e^{i\omega x} - 1) + \ldots\right] & \text{for } \Delta t > 0 \end{cases} \quad (B.11)$$

where R' represents the temperature derivative of R. In those expressions, the sample temperature, T_s, and the melting points, T_m, have been changed to variables t and t_0 having the dimension of time, and $\Delta t \equiv t - t_0$ represents the difference which is a measure of the superheating ΔT,

$$T_s = \beta t + \tilde{T}_s e^{i\omega t} \quad (B.12)$$

$$T_m = \beta t_0 + \tilde{T}_s e^{i\omega t_0} \quad (B.13)$$

$$\Delta T \equiv T_s - T_m = \beta\Delta t + \tilde{T}_s e^{i\omega t_0}(e^{i\omega\Delta t} - 1) \quad (B.14)$$

Accordingly, Fourier transform, $G(\omega')$, is represented as,

$$G(\omega') = i\omega'\Delta H \int_{-\infty}^{\infty} dt\, e^{-i\omega' t}\int_{\infty}^{\infty} dT_m \phi(t, T_m)$$

$$= i\omega'\Delta H \int_0^\infty dt_0(\beta + i\omega\tilde{T}_s e^{i\omega t_0})e^{-i\omega' t_0}\phi_0(t_0) \times \int_{-\infty}^{\infty} d(\Delta t)e^{-i\omega'\Delta t}\psi(\Delta t) \quad (B.15)$$

Fourier transform of the underlying heat flow $\overline{F}_{melt}$ is then given as,

$$\overline{G}(\omega') = \Delta H \int_0^\infty \beta dt_0 e^{-i\omega' t_0}\phi_0(t_0) i\omega' \times \int_{-\infty}^{\infty} d(\Delta t)e^{-i\omega'\Delta t}\overline{\psi}(\Delta t)$$

$$= \Delta H G_{\phi 0}(\omega')G_{\overline{\dot{\psi}}}(\omega') \quad (B.16)$$

Here, $G_{\phi 0}$ represents Fourier transform of $\phi_0(t_0)$ and $G_{\overline{\dot{\psi}}}$ Fourier transform of the time derivative of $\overline{\psi}$ defined as,

$$\overline{\psi}(\Delta t) \equiv \begin{cases} 1 & \text{for } \Delta t < 0 \\ e^{-\int_0^{\Delta t} dx R(\beta x)} & \text{for } \Delta t > 0 \end{cases} \quad (B.17)$$

Eq. (B.16) means that the underlying heat flow, $\overline{F}_{melt}(t)$, is given by the convolution of $\phi_0(t_0)$ and $\psi(\Delta t)$ represented as,

$$\overline{F}_{melt}(t) = \Delta H \int_0^\infty \beta dt_0 \phi_0(t_0)\overline{\dot{\psi}}(t - t_0) \quad (B.18)$$

On the other hand, Fourier transform of the modulation component, $G'_T(\omega', \omega)$, is given as,

$$G'_T(\omega', \omega) = i(\omega' + \omega)\Delta H G_{\phi 0}(\omega') \times \left\{ \frac{i\omega}{\beta} G_{\overline{\dot{\psi}}}(\omega' + \omega) - \int_0^\infty d(\Delta t)e^{-i(\omega' + \omega)\Delta t} e^{-\int_0^{\Delta t} dx R(\beta x)} \times \int_0^{\Delta t} dx R'(\beta x)(e^{i\omega x} - 1) \right\} \quad (B.19)$$

Now, we can discuss the condition for $G'_T(\omega', \omega)$ given by Eq. (B.7). The condition is satisfied when $G_{\phi_0}(\omega')$ becomes negligible outside the range of $\omega' \ll \omega$ and $\omega'\tau \ll 1$, as we see with the two examples of the

melting rate coefficient of R_0 and $R_1(\Delta T)$ in the following. The condition of the quasi-steady state is then expressed in the following manner when translated to the corresponding temperature range,

(Temperature range in which the change in $\phi_0(T_m)$ is negligible)

$$\gg \beta \times (\text{period of modulation}) \tag{B.20}$$

and

$$\gg 2\pi\beta\tau \tag{B.21}$$

4.1. Constant R_0 for $\Delta T>0$

$G'_T(\omega', \omega)$ is calculated as,

$$G'_T(\omega', \omega) = \frac{i\omega}{\beta}\Delta H G_{\phi 0}(\omega')\frac{-1}{1 + i(\omega' + \omega)\tau_0} \tag{B.22}$$

Eq. (B.22) can be approximated as the following form satisfying the condition of Eq. (B.7), when the frequency range concerned satisfies the condition of $\omega' \ll \omega$ or $(\omega'\tau)\ (\omega\tau) \ll 1$,

$$\frac{i}{\omega}G'_T(\omega', \omega) = g_0(\omega')\frac{1}{1 + i\omega\tau_0} \tag{B.23}$$

The dependence on ω shown in Eq. (B.23) is actually correspondent to that of Eq. (A.11) obtained under the assumption of $\phi_0(T_m)=\phi_0$.

4.2. $R=a\Delta T$

When the frequency range satisfies $\omega' \ll \omega$, Eq. (B.19) can be approximated as,

$$G'_T(\omega', \omega) = \frac{i\omega}{\beta}\Delta H G_{\phi 0}(\omega')\frac{1}{\omega\tau_1} \times \left\{\omega'\tau_1 + i\frac{\sqrt{\pi}}{2} - ie^{-(\omega\tau_1)^2}\left(\frac{\sqrt{\pi}}{2} - i\int_0^{\omega\tau_1} e^{x^2}dx\right) \times [1 + 2(\omega'\tau)(\omega\tau)]\right\} \tag{B.24}$$

If the frequency range further satisfies $(\omega'\tau)\ (\omega\tau) \ll 1$ (namely, $\omega'\tau \ll 1$), $G'_T(\omega', \omega)$ can be modified to satisfy the condition of Eq. (B.7) as,

$$\frac{i}{\omega}G'_T(\omega', \omega) = g_1(\omega')\frac{1}{\omega\tau_1}\left[e^{-(\omega\tau_1)^2}\int_0^{\omega\tau_1} e^{x^2}dx \times -i\frac{\sqrt{\pi}}{2}(1 - e^{-(\omega\tau_1)^2})\right] \tag{B.25}$$

Its dependence on ω also corresponds to that of Eq. (A.14).

References

[1] A. Toda, T. Oda, M. Hikosaka, Y. Saruyama, Polymer 38 (1997) 231–233.
[2] A. Toda, T. Oda, M. Hikosaka, Y. Saruyama, Thermochim. Acta 293 (1997) 47–64.
[3] A. Toda, C. Tomita, M. Hikosaka, Y. Saruyama, Polymer 38 (1997) 2849–2852.
[4] A. Toda, C. Tomita, M. Hikosaka, Y. Saruyama, Polymer in press.
[5] A. Toda, C. Tomita, M. Hikosaka, Y. Saruyama, Polymer submitted.
[6] P.S. Gill, S.R. Sauerbrunn, M. Reading, J. Therm. Anal. 40 (1993) 931–939.
[7] M. Reading, D. Elliott, V.L., Hill, J. Therm. Anal., 40 (1993) 949–955.
[8] M. Reading, A. Luget, R. Wilson, Thermochim. Acta 238 (1994) 295–307.
[9] B. Wunderlich, Y. Jin, A. Boller, Thermochim. Acta 238 (1994) 277–293.
[10] A. Boller, Y. Jin, B. Wunderlich, J. Therm. Anal. 42 (1994) 307–330.
[11] I. Hatta, Jpn. J. Appl. Phys. 33 (1994) L686.
[12] N.O. Birge, S.R. Nagel, Phys. Rev. Lett. 54 (1985) 2674–2677.
[13] A. Hensel, J. Dobbertin, J.E.K. Schawe, A. Boller, C. Schick, J. Therm. Anal. 46 (1996) 935–954.
[14] B. Wunderlich, Macromolecular Physics, Academic Press, New York, 1976, vol. 3.
[15] I. Okazaki, B. Wunderlich, Macromolecules 30 (1997) 1758–1764.
[16] K. Ishikiriyama, B. Wunderlich, J. Polym. Sci., B, Polym. Phys. Ed. 35 (1997) 1877.
[17] E. Hellmuth, B. Wunderlich, J. Appl. Phys. 36 (1965) 3039.
[18] U. Gaur, B. Wunderlich, J. Phys. Chem. Ref. Data 10 (1981) 119.
[19] M. Nishikawa, Y. Saruyama, Thermochim. Acta 267 (1995) 75–81.
[20] Y. Saruyama, Thermochim. Acta, in press.
[21] Y. Saruyama, J. Therm. Anal. 49 (1997) 139–142.
[22] M.J. Vold, Anal. Chem. 21 (1949) 683–688.